ACS OMEGA

http://pubs.acs.org/journal/acsodf

Article

High-Throughput Screening Identifies Synthetic Peptides with Antibacterial Activity against *Mycobacterium abscessus* and Serum Stability

Natalie Iannuzo, Yannik A. Haller, Michelle McBride, Sabrina Mehari, John C. Lainson, Chris W. Diehnelt,* and Shelley E. Haydel*

Cite This: *ACS Omega* 2022, 7, 23967−23977

Read Online

ACCESS | Metrics & More | Article Recommendations | Supporting Information

ABSTRACT: The rise in antibiotic resistance in bacteria has spawned new technological approaches for identifying novel antimicrobials with narrow specificity. Current antibiotic treatment regimens and antituberculosis drugs are not effective in treating *Mycobacterium abscessus*. Meanwhile, antimicrobial peptides are gaining prominence as alternative antimicrobials due to their specificity toward anionic bacterial membranes, rapid action, and limited development of resistance. To rapidly identify antimicrobial peptide candidates, our group has developed a high-density peptide microarray consisting of 125,000 random synthetic peptides screened for interaction with the mycobacterial cell surface of *M. abscessus* morphotypes. From the array screening, peptides positive for interaction were synthesized and their antimicrobial activity was validated. Overall, six peptides inhibited the *M. abscessus* smooth morphotype (IC_{50} = 1.7 μM for all peptides) and had reduced activity against the *M. abscessus* rough morphotype (IC_{50} range: 13−82 μM). Peptides ASU2056 and ASU2060 had minimum inhibitory concentration values of 32 and 8 μM, respectively, against the *M. abscessus* smooth morphotype. Additionally, ASU2060 (8 μM) was active against *Escherichia coli*, including multidrug-resistant *E. coli* clinical isolates, *Pseudomonas aeruginosa*, and methicillin-resistant *Staphylococcus aureus*. ASU2056 and ASU2060 exhibited no significant hemolytic activity at biologically relevant concentrations, further supporting these peptides as promising therapeutic candidates. Moreover, ASU2060 retained antibacterial activity after preincubation in human serum for 24 h. With antimicrobial resistance on the rise, methods such as those presented here will streamline the peptide discovery process for targeted antimicrobial peptides.

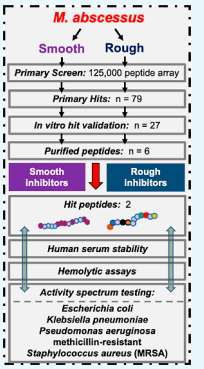

INTRODUCTION

Antimicrobial resistance is a growing threat aggravated by the high cost and long duration of few viable treatment options available for resistant life-threatening infections.[1] While the incidence of resistant infections is increasing, discoveries of novel targets for antimicrobials have declined since the 1970s.[1,2] Even with new incentives offered in 2010 to spur antibiotic development and FDA approval, only one out of the eight antimicrobials approved between 2010 and 2015 employed a novel mechanism of action.[3]

Antimicrobial peptides (AMPs) have been discovered in a diversity of organisms and have correspondingly diverse structures and specificities. Interest has increased in AMPs due to their selectivity toward anionic bacterial cell membranes, rapid action, and lack of developed resistance.[4−6] Since AMPs are increasingly considered as therapeutics, they are often designed and optimized with amino acid substitutions to be cationic and amphipathic with the goal of either lysing bacteria or inhibiting bacterial growth via disruption of cell wall, DNA, RNA, and/or protein synthesis.[7−9] Moreover, novel AMP mechanisms may be discovered from screening random, synthetic peptides for antimicrobial activity. As the need for antimicrobials effective against resistant organisms intensifies, so must the pace of discovery methods. The discovery and development of novel AMPs will fill this gap in vital therapeutic options.

Mycobacteria other than *Mycobacterium tuberculosis* and *Mycobacterium leprae* are referred to as nontuberculous mycobacteria (NTM).[10,11] *Mycobacterium abscessus* (*Mabs*), the third most frequently recovered respiratory NTM in the United States, is one of the most clinically challenging NTM infections and accounts for 65−80% of rapidly growing NTM isolates.[12−14] Two distinct morphotypes of *Mabs* subsp. *abscessus* are distinguishable on solid media: a smooth (S), biofilm-forming, noncording variant and a rough (R), non-biofilm-forming, cording variant.[15,16] Clinically, the S variant colonizes the lung, while the R variant appears after initial colonization and is more virulent, more resistant to macrophage killing, and is associated with more severe and persistent pulmonary infections.[15,17−25] *Mabs* resistance to classical

Received: May 7, 2022
Accepted: June 8, 2022
Published: June 27, 2022

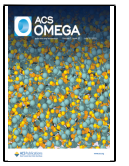

antituberculosis drugs and current antibiotics leads to a lack of effective drug regimens,[12,15] and *Mabs* pulmonary infections have no known effective drug treatments.[26] The American Thoracic Society recommends macrolides (clarithromycin and azithromycin), in combination with intravenous amikacin and cefoxitin (or imipenem) for at least 1 year until sputum samples are culture negative,[12,27,28] yet *Mabs* infections respond poorly to macrolides. The only known cure for *Mabs* pulmonary disease is surgical lung resection and concurrent multidrug therapy.[29,30] Antibiotic regimens are often associated with adverse side effects, and although antibiotics can improve symptoms, *Mabs* infections have an estimated 50% recurrence rate.[31,32]

For the treatment of NTM pulmonary infections, AMPs are more potent and have fewer side effects than orally and intravenously administered antibiotics and can be delivered as an inhaled therapeutic.[14] In addition, inhaled AMPs, similar to inhaled small molecule antibiotics, do not cross the respiratory epithelium and therefore reduce off-target effects and increase lung bioavailability.[33] While there are currently no naturally occurring peptides or their derivatives recommended to treat *Mabs* infections,[26] novel approaches to eradicating the disease are needed due to *Mabs*' acquired and intrinsic resistance to classical antituberculous drugs, most small molecule antibiotics, and disinfectants.[34,35]

Our group has produced high-density (HD) peptide microarrays of up to 330,000 random peptides using in situ synthesis, where photolithographic masks are employed to illuminate discrete features on a silicon wafer coated with a photoresist and a photoacid generator.[36] We used this method to produce new libraries with fewer synthetic peptides in larger spots while maintaining the same slide geometry compatible with a standard 96-well microtiter plate.[36] Peptides are 17-mers and are synthesized from 15 different amino acids, including D-versions of Lys, Arg, Ala, Leu, and Trp. Previously, we developed an AMP discovery method using spotted peptide microarrays of 10,000 peptides to identify peptides that bind to targeted bacteria.[37−39] In this study, a 125,000 HD peptide microarray was used to screen for peptides with in vitro binding activity against *Mabs* S and R morphotypes. We then evaluated the activity of candidate peptides using a series of microdilution antimicrobial susceptibility assays performed in three culture media with and without a chelating agent. The cytotoxicity of identified *Mabs* inhibitory peptides was evaluated using human red blood cell (hRBC) hemolytic assays. Activity against additional Gram-positive and Gram-negative organisms was assessed to determine the specificity of peptide antimicrobial activity.

For pathogens without effective drug treatments, such as *Mabs*, high-throughput therapeutic discovery methods are critical to improve the cost and speed of uncovering effective antimicrobials. Here, such a method is demonstrated; the synthesized random peptides were screened against *Mabs* with positive hits tested for in vitro inhibitory activity. Importantly, inhibitory peptides were identified, and preliminary tests indicate minimal toxicity.

MATERIALS AND METHODS

***Mabs* Strains and Growth Conditions.** *Mabs* ATCC 19977 S morphotype (*Mabs* 19977S) cells were cultured at 37 °C in Middlebrook 7H9 supplemented with albumin, dextrose, and catalase (ADC) (10%), Tween 80 (0.05%), and glycerol (0.2%) (herein referred to as M7H9). *Mabs* 19977S was exposed to clarithromycin (8 μg/mL) in M7H9 for 24 h at 37 °C, subjected to serial dilutions, and plated on Middlebrook 7H10 agar supplemented with oleic acid, ADC (OADC) (herein referred to as M7H10). After a five-day incubation at 37 °C, a single, isolated colony displaying a rough morphotype (*Mabs* 19977R) was detected, grown, and stored at −70 °C. *Mabs* 19977S and *Mabs* 19977R were grown for approximately 32 h at 37 °C, diluted 1:100 in fresh, prewarmed M7H9, and grown for an additional 14 h until the cultures reached early logarithmic phase (OD_{600} = 0.2−0.3).

***Pseudomonas aeruginosa*, *Escherichia coli*, *Klebsiella pneumoniae*, and Methicillin-Resistant *Staphylococcus aureus* Strains and Growth Conditions.** *P. aeruginosa* (ATCC 27853) and methicillin-resistant *S. aureus* (MRSA) USA300 were cultured at 37 °C in tryptic soy broth (TSB). *E. coli* (ATCC 25922) and *K. pneumoniae* (ATCC 13883) cells were cultured in Luria broth (LB). After incubation (16 h), *P. aeruginosa*, *E. coli*, and *K. pneumoniae* cultures were centrifuged (3715*g*) for 3 min, resuspended in sterile 0.9% saline, and adjusted to OD_{600} of 0.4, 0.07, and 0.1 for *P. aeruginosa*, *E. coli*, and *K. pneumoniae*, respectively. MRSA was cultured at 37 °C in TSB for 18 h before centrifugation at 3715*g* for 3 min. MRSA was then resuspended in Mueller Hinton Broth (MHB) and diluted to an OD_{600} of 0.1 in sterile 0.9% saline. Bacterial preparations were serially diluted in MHB to approximately 10^5 CFU/mL for use in the assays.

***E. coli* Clinical Isolates.** Deidentified excess and residual clinical urine samples were obtained from the clinical microbiology laboratory at Mayo Clinic Hospital, Phoenix, Arizona (approved by Mayo Clinic Biospecimen Subcommittee BIO00015462).[40−42] *E. coli* urinary tract infection clinical isolates were cultured as described above and stored in 15-20% glycerol at −70 °C.

Peptide Microarrays. The HD peptide microarrays were synthesized in house with a library of peptides on a silicon wafer coated with a photoresist and a photoacid generator, according to our published methods.[36] Micron-scale regions of photoacid are generated and exposed to protected amino acids. If acid is present, the amino acid is deprotected and coupled. Through subsequent steps, peptides are synthesized, forming a microarray of 123,816 peptides with unique sequence compositions. Replicate peptide microarrays are produced in a standard microscope slide-sized format[36] with a geometry that is compatible with a standard 96-well microtiter plate, thereby enabling standard robotics and plate washers to be used for the binding assays. Prior to screening, slides were placed in a four-slide chamber (ArrayIt, Sunnyvale, CA) and blocked for 1 h in 150 μL of 3% bovine serum albumin (BSA) in phosphate-buffered saline (PBS), pH 7.4 with 0.05% Tween 20 (PBST) and agitation (300 rpm). Slides were washed three times in PBST using a plate washer (Beckman Coulter Biomek, Indianapolis, IN).

***Mabs* Screening on Peptide Microarrays.** *Mabs* cultures were prepared as described above, centrifuged, and washed three times in PBST. Two biological replicates of *Mabs* 19977S or *Mabs* 19977R cells (~1.0×10^8 CFU/mL) were labeled with 200 μg of AF647-NHS (ThermoFisher Scientific, Carlsbad, CA) in prewarmed PBST. Two biological replicates of *Mabs* 19977S or *Mabs* 19977R cells (~3×10^8 CFU/mL) were labeled with 50 μg of cell tracker orange (CTO) CMRA (ThermoFisher Scientific) in prewarmed PBST. Cells were incubated with AF647 or CTO for 1 h at room temperature or 37 °C, respectively, with shaking at 250 rpm. Fluorescently labeled bacterial cells were washed, resuspended in 3% BSA in PBST to achieve a concentration of ~10^8 CFU/mL, and diluted to 1 ×

https://doi.org/10.1021/acsomega.2c02844
ACS Omega 2022, 7, 23967−23977

10^7 CFU/mL in a 96-well microtiter plate. The cells were transferred to the slide chamber at 150 μL per well and incubated on a shaker (ThermoMixer, Eppendorf, Hauppauge, NY) for 1 h at 37 °C at 300 rpm. The slide was washed three times in PBST, three times in water, dried, and scanned on an Innoscan 900AL microarray scanner (Innopsys, Carbonne, France). Data were analyzed using GenePix, and raw data files were analyzed using Microsoft Excel and JMP statistical software (Cary, NC).

Identification of Peptides with Activity against *Mabs*. Bacteria grown in M7H9, MHB, and cation-adjusted MHB (CAMHB) were used to identify unpurified peptides with inhibitory activity against *Mabs* 19977S and *Mabs* 19977R. The initial 27 peptides (50−65% purity) were synthesized by Sigma-Aldrich (St. Louis, MO) PEPscreen Custom Peptide Libraries. *Mabs* ATCC 19977S and ATCC 19977R mid-logarithmic-phase cultures (OD_{600} 0.5−0.6) were centrifuged (3715*g*) for 2 min, washed in prewarmed M7H9, resuspended in M7H9, MHB, or CAMHB, and diluted to 10^6 CFU/mL. In a 96-well polystyrene microtiter plate, media (M7H9, MHB, or CAMHB), unpurified peptides (100 or 10 μM), ethylenediaminetetraacetic acid (EDTA) (100 μM), and cells (*Mabs* 19977S or *Mabs* 19977R) (10^5 CFU/mL) were added. EDTA was added to determine if metal ion chelation would alter peptide activity. Clarithromycin (4 μg/mL) was used as an antibiotic positive control. The 96-well microtiter plates were statically incubated at 37 °C for 72 h. The OD_{600} was measured every 24 h using a SpectraMax M2 microplate reader (Molecular Devices, San Jose, CA, USA). Peptides that reduced *Mabs* growth by ≥50%, when compared to the growth control OD_{600}, were considered active.

***Mabs* Microdilution Antimicrobial Assays with Purified Peptides.** The six peptides with activity against *Mabs* were synthesized and high-performance liquid chromatography-purified by WatsonBio Sciences: ASU2001—98%; ASU2009—99%; ASU2019—90%; ASU2056—95%; ASU2059—100%; and ASU2060—99%. To determine effects on *Mabs* viability, microdilution antimicrobial assays were performed in MHB. *Mabs* 19977S and *Mabs* 19977R mid-logarithmic-phase cultures (OD_{600} 0.5−0.6) were prepared and processed as described above. In a 96-well microtiter plate, MHB, two-fold serial dilutions (256−2 μM) of purified peptides, EDTA (100 μM), and cells (*Mabs* 19977S or *Mabs* 19977R) (10^5 CFU/mL) were added. Clarithromycin (4 μg/mL) was used as an antibiotic positive control. Microtiter plates were statically incubated at 37 °C for 96 h. The OD_{600} was measured every 24 h using a SpectraMax M2 microplate reader (Molecular Devices, San Jose, CA, USA).

Identification of Peptides with Cross-Inhibitory Activity against *P. aeruginosa*, *E. coli*, *K. pneumoniae*, and MRSA. *P. aeruginosa*, *E. coli*, *K. pneumoniae*, and MRSA cultures were grown overnight and diluted to 10^6 CFU/mL prior to initiating experiments. In a 96-well polystyrene microtiter plate, MHB, purified peptides [at their respective minimum inhibitory concentration (MIC) values against *Mabs*], EDTA (100 μM), and cells (*P. aeruginosa*, *E. coli*, *K. pneumoniae*, or MRSA) (10^5 CFU/mL) were added. Amikacin (6 and 3 μg/mL), vancomycin (8 and 4 μg/mL), and ampicillin (32 and 16 μg/mL) were used as antibiotic controls. The 96-well microtiter plates were statically incubated at 37 °C for 24 h after which samples from each well were subjected to serial dilutions in sterile 0.9% saline and plated on MHA in duplicate. Colonies were counted to determine viability.

Determination of ASU2060 MIC against *E. coli* Clinical Isolates. The MICs of ciprofloxacin, cefazolin, ampicillin, and nitrofurantoin against the *E. coli* clinical isolates were determined in triplicate to establish antibiotic susceptibility profiles for each isolate (n = 6). To determine the MIC of antibiotics and ASU2060, isolates were cultured in LB for 16 h, centrifuged (3715*g*) for 1 min, resuspended in MHB, and diluted to ~10^7 CFU/mL (OD_{600} = 0.05). Samples were serially diluted in MHB to ~10^5 CFU/mL and added to a 96-well polystyrene plate prepared with ASU2060 (128−4 μM). After incubation for 22 h at 37 °C, the OD_{600} was measured using a SpectraMax M2 microplate reader (Molecular Devices, San Jose, CA, USA). Values were normalized to the medium blank (MHB) and *E. coli* (ATCC 25922) treated with nitrofurantoin at 64 μM.

Cytotoxicity Assessment of *Mabs* Inhibitory Peptides. To determine if the purified, *Mabs* inhibitory peptides were toxic, hRBC hemolytic assays were performed. Peptides (at 1X, 2X, and 4X their respective *Mabs* 19977S MICs) were added to 4% hRBC in saline and statically incubated for 1 h or 18 h at 37 °C. Triton X-100 (1%) was used as a positive control and resulted in complete hRBC lysis. Following incubation, the peptide-hRBC mixtures and the 1% Triton X-100 positive controls were centrifuged for 1 min at 1000*g* to pellet the intact hRBC. The supernatant for each experimental mixture and control was removed, and OD_{475} measurements were recorded to determine the percentage of lysed hRBC. The percentage of hemolytic activity was normalized by comparing the supernatant absorbance of all conditions tested to an equivalent number of hRBC lysed with 1% Triton X-100 (eq 1).

$$\text{Percent cytotoxicity} = \frac{OD_{475}\ \text{experimental mixture supernatant}}{OD_{475}\ \text{positive control supernatant}} \times 100\% \quad (1)$$

Serum Stability Assays. The collection and use of all human serum for research presented here were approved by the Institutional Review Board of Arizona State University, protocol no. 0912004625. Informed consent was obtained from all human subjects. Blood was collected from five healthy donors, and the serum was separated. Serum samples were pooled and stored at −70 °C prior to experimental use. ASU2060 was incubated with 20% pooled, human serum for various intervals (1−24 h). At each time point, sample aliquots were removed and mixed with complete, EDTA-free protease inhibitor (11873580001, Roche, Indianapolis, IN). ASU2060 serum stability was determined by examining retained biological activity in bactericidal assays with *E. coli* ATCC 25922 (~2 × 10^5 CFU/mL).

Statistical Analyses. All experiments were performed in triplicate. Statistical significance was determined using linear regression analyses with $p < 0.05$. All analyses were performed with GraphPad Prism software Version 9.0.2.

RESULTS

***Mabs* ATCC 19977 Rough Variant.** Despite similar S and R morphotype susceptibility to clarithromycin, amikacin, and cefoxitin,[43] differences in virulence and host−pathogen interactions prompted us to screen for active peptides against both *Mabs* S and R variants. After exposure of *Mabs* 19977S to clarithromycin, a subpopulation of cells frequently exhibited a rough morphology phenotype on M7H10 agar without

https://doi.org/10.1021/acsomega.2c02844
ACS Omega 2022, 7, 23967−23977

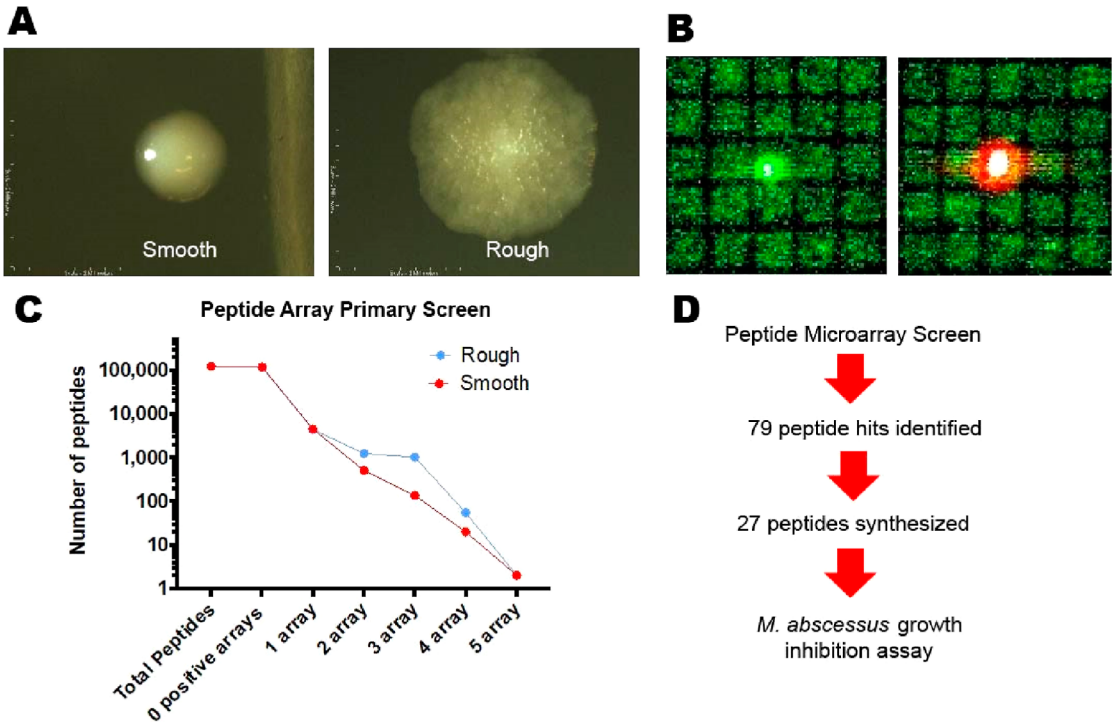

Figure 1. (A) Representative colonies of *Mabs* ATCC 19977S and *Mabs* ATCC 19977R morphotypes. (B) CTO-labeled (left) or AF647-labeled (right) *Mabs* ATCC 19977S binding to a peptide spot on the microarray. (C) Statistics of bacteria-binding signals to the peptide microarrays. (D) Workflow to select and test *Mabs* peptides.

antibiotics (Figure 1A). The rough variant, *Mabs* 19977R, did not revert to a smooth morphotype and was stably maintained during in vitro growth (18−24 h), thereby allowing peptide microarray screening of both *Mabs* 19977S and *Mabs* 19977R cells.

High-Throughput Screening: *Mabs* Morphotype Binding on HD Peptide Microarrays. *Mabs* 19977S or *Mabs* 19977R cells were labeled with either amine-reactive Alexa Fluor 647 (AF647), which binds and fluoresces the cell surface, or CTO, which fluoresces after internalization into the cytoplasm, and incubated on replicate peptide microarrays (n = 12). One notable adaptation from spotted peptide microarrays to the in situ synthesized HD peptide microarrays is the reduction in spot size. The HD microarrays have smaller features (14 × 14 μm squares) than spotted peptide microarrays (~80 μm diameter circles),[37] reducing the number of bacteria that can bind a given spot (Figure 1B). In previous studies, bacteria bound to a given peptide spot revealed several thousand relative fluorescence units (RFUs), while signals were close to background for nonbinding peptides.[37] While there were few *Mabs* bacteria bound to a single peptide feature, the use of 12 replicate arrays per condition enabled a counting approach to be used for peptide hit identification. Essentially, by counting the number of times a peptide bound *Mabs* across the 12 replicate arrays, a relative measure of peptide binding for each *Mabs* morphotype was obtained (Figure 1C). By defining bacterial binding as RFU > 10 times the array median signal for AF647 or CTO and counting the number of times a given peptide was positive for the 12 morphotype replicates, a small number of peptides (n = 79) were positive in four or more arrays per morphotype. From these peptides, we selected 27 peptides for synthesis and subsequent testing based upon array reactivity and peptide properties (Figure 1D).

Identification of Synthetic Peptides with Activity against *Mabs* during Growth in M7H9, MHB, and CAMHB. To evaluate if the 27 synthetic peptides had in vitro activity, *Mabs* 19977S and *Mabs* 19977R were incubated with the peptides at 100 and 10 μM, with or without EDTA (100 μM), in M7H9 broth, MHB, and CAMHB for 96 h. In M7H9 broth, five peptides (ASU2001, ASU2009, ASU2019, ASU2056, and ASU2059; 100 μM) exhibited activity against both morphotypes when EDTA was added (Figure 2A). Additionally, four peptides (ASU2060, ASU2061, ASU2062, and ASU2070; 100 μM) were active against the *Mabs* 19977S smooth morphotype only, when EDTA was added (Figure 2A). When EDTA was not added, the smooth-acting peptides (ASU2060, ASU2061, ASU2062, and ASU2070; 100 μM) displayed less activity (Figure 2B). One peptide (ASU2001; 100 μM) exhibited activity against the *Mabs* 19977R rough morphotype in the presence and absence of EDTA (Figure 2A,B). In culture medium with cation supplementation (CAMHB), ASU2060 (100 μM) had activity against both morphotypes when EDTA was added (Figure 2C). ASU2060 (100 μM) inhibited the *Mabs* 19977S smooth morphotype in CAMHB without EDTA (Figure 2D). In MHB, fourteen peptides (100 μM) exhibited activity against both morphotypes when EDTA was added (Figure 2E). Five of the fourteen peptides (ASU2001, ASU2009, ASU2019, ASU2056, and ASU2059) that had activity against both morphotypes in M7H9 maintained activity in MHB when EDTA was added (Figure 2E). Three of the four smooth-acting peptides (ASU2061, ASU2062, and ASU2070) (100 μM) that had activity in M7H9 with EDTA maintained inhibitory activity in MHB when EDTA was added (Figure 2E). Without EDTA supplementation, none of the peptides displayed activity against *Mabs* in MHB (Figure 2F). At lower concentrations (10 μM), peptides lacked activity against *Mabs* 19977S and *Mabs* 19977R morphotypes in M7H9 broth,

https://doi.org/10.1021/acsomega.2c02844
ACS Omega 2022, 7, 23967−23977

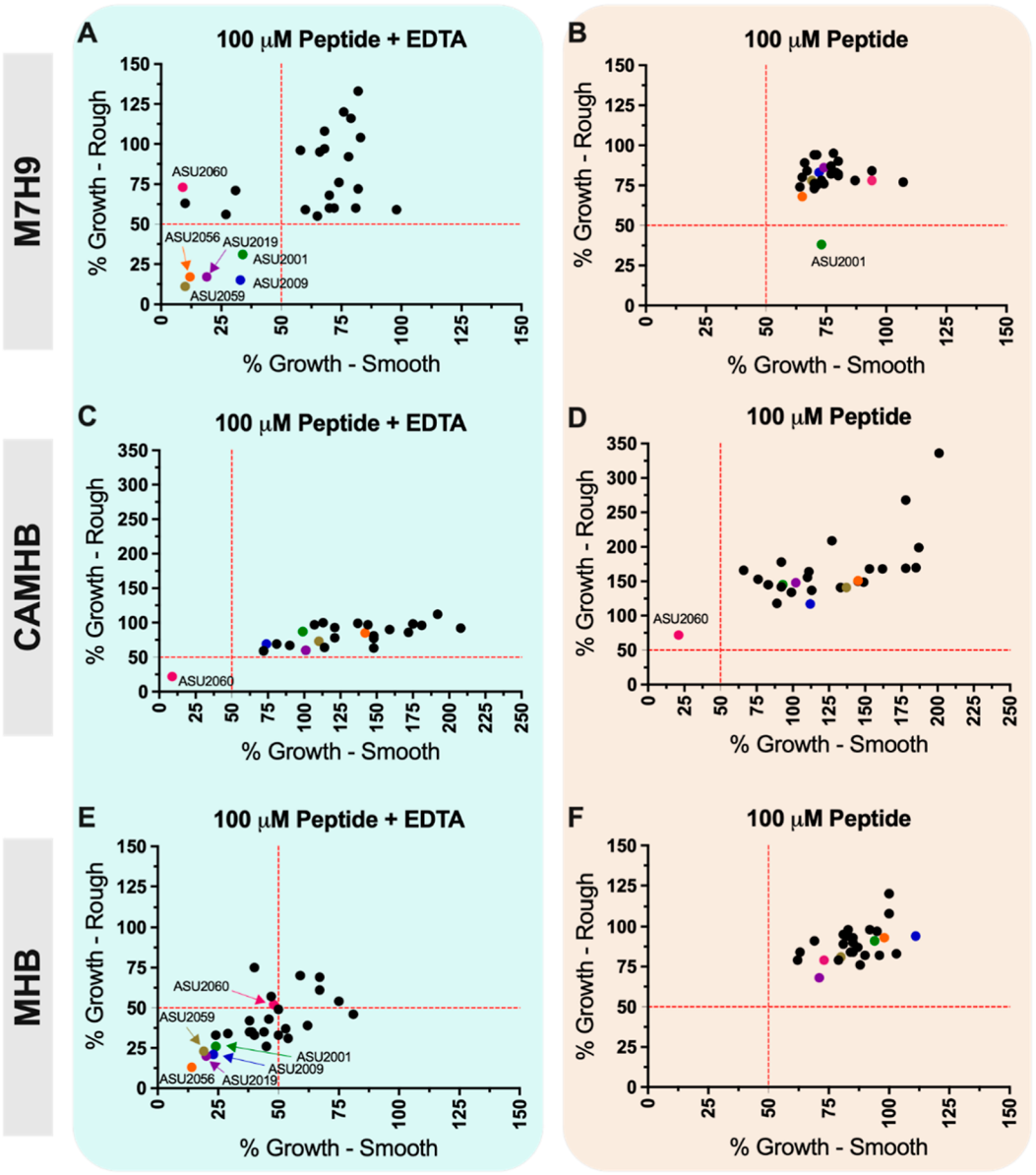

Figure 2. Growth inhibition assays with the 27 peptides that interacted with *Mabs* during the peptide microarray screening. MIC assays with *Mabs* 19977S and *Mabs* 19977R were performed in (A,B) M7H9, (C,D) CAMHB, or (E,F) MHB with peptide (100 μM) and EDTA (100 μM) or peptide (100 μM) alone. All experiments were incubated at 37 °C for 72 h. Peptides that reduced *Mabs* growth by ≥50% (red hatched lines), when compared to the growth control OD_{600}, were considered active. Panels highlight six peptides with consistent inhibitory activity against *Mabs* 19977S and *Mabs* 19977R in different media. ASU2001—green circles; ASU2009—blue circles; ASU2019—purple circles; ASU2056—orange circles; ASU2059—olive green circles; and ASU2060—red circles. All experiments were performed in triplicate with the average of all three replicates plotted for each peptide.

CAMHB, or MHB regardless of EDTA supplementation (Supporting Information, Figure S1).

***Mabs* Microdilution Inhibitory Assays with Purified Peptides.** The six peptides (ASU2001, ASU2009, ASU2019, ASU2056, ASU2059, and ASU2060) with activity against *Mabs* were synthesized, purified (see Materials and Methods), and subjected to *Mabs* microdilution inhibitory assays in MHB, with EDTA (100 μM), for 96 h. From these assays, ASU2001, ASU2009, ASU2019, and ASU2059 had IC_{50} values <1.8 μM and MIC values of 256 μM against *Mabs* 19977S (Figure 3A–C,E). ASU2056 and ASU2060 peptides displayed the greatest potency against *Mabs* 19977S with MIC values of 32 and 8 μM, respectively (Figure 3D,F). Against *Mabs* 19977R, the six peptides displayed calculated IC_{50} values that were 8–46 times higher than against *Mabs* 19977S (Figure 4). ASU2001, ASU2019, and ASU2059 peptides revealed IC_{50} values of 76–82 μM against *Mabs* 19977R (Figure 4A,C,E), while ASU2009 and ASU2056 IC_{50} values were lower at 52 and 45 μM, respectively (Figure 4B,D). Like *Mabs* 19977S, ASU2060 displayed greatest potency against *Mabs* 19977R with an IC_{50} value of 13 μM (Figure 4F). MICs for all purified peptides against *Mabs* ATCC19977S and *Mabs* ATCC19977R are listed in Table 1. Based on the results from the high-throughput HD peptide arrays of 123,816 randomly synthesized peptides and all *Mabs* microdilution inhibitory assays, two promising hit peptides, ASU2056 and ASU2060, were selected for additional experiments. Notably, not all potential AMP hits were pursued.

https://doi.org/10.1021/acsomega.2c02844
ACS Omega 2022, 7, 23967–23977

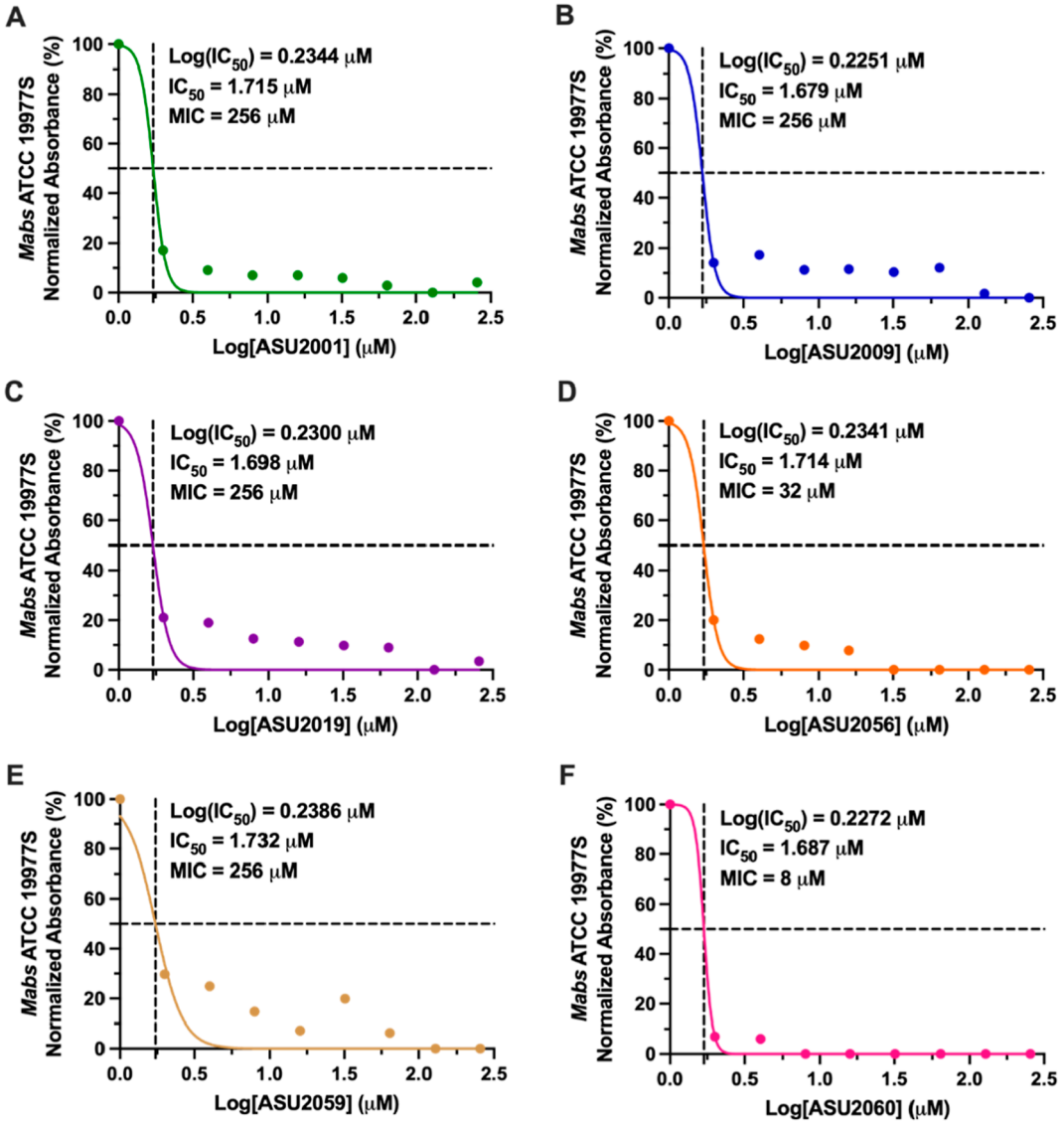

Figure 3. IC_{50} and MIC values of (A) ASU2001, (B) ASU2009, (C) ASU2019, (D) ASU2056, (E) ASU2059, and (F) ASU2060 peptides against *Mabs* ATCC 19977S smooth morphotype in MHB supplemented with EDTA (100 μM) for 96 h at 37 °C. Three independent experiments were performed with the average of all three replicates plotted for each peptide. Absorbance (OD_{600}) values were normalized to the growth control (100%), and IC_{50} values were determined by nonlinear regression.

Peptide Inhibitory Activity against *E. coli*, *P. aeruginosa*, *K. pneumoniae*, and MRSA USA300 during MHB Growth. To determine if ASU2056 (32 μM; *Mabs* MIC) and ASU2060 (8 μM; *Mabs* MIC) have in vitro activity against other microorganisms of interest, *E. coli*, *P. aeruginosa*, *K. pneumoniae*, and MRSA USA300 cells were incubated with the peptides in MHB with and without EDTA (100 μM) for 24 h. Without EDTA supplementation, ASU2056 lacked activity against the four bacteria (Figure 5A). In the presence of EDTA, ASU2056 inhibited *E. coli* at 16 and 32 μM concentrations but did not alter *P. aeruginosa*, *K. pneumoniae*, or MRSA growth (Figure 5B). ASU2060 displayed bactericidal activity against *E. coli* at concentrations of 8 and 4 μM in the absence and presence of EDTA, respectively (Figure 5C,D). ASU2060 (8 μM), without EDTA, inhibited *P. aeruginosa* (Figure 5C) but lacked *P. aeruginosa* activity in the presence of EDTA (Figure 5D). Conversely, ASU2060 (8 μM) with EDTA inhibited MRSA (Figure 5D) but lacked MRSA activity in the absence of EDTA (Figure 5C). Neither ASU2056 nor ASU2060 had activity against *K. pneumoniae* (Figure 5). Collectively, the two promising anti-*Mabs* hit peptides, ASU2056 and ASU2060, also inhibit or kill *E. coli*, *P. aeruginosa*, and MRSA.

ASU2056 and ASU2060 Peptides Lack hRBC Hemolytic Activity. To determine if the ASU2056 and ASU2060 exhibit eukaryotic cell toxicity, the two peptides were evaluated via hRBC hemolytic assays. The peptides were incubated with 4% hRBC for 1 h and 18 h at 1X, 2X, and 4X of their *Mabs* 19977S MIC values. When the ASU2056 and ASU2060 peptides were incubated for 18 h at 4X MIC concentrations of 128 and 32 μM, respectively, hRBC hemolysis averaged less than 1%, suggesting that the peptides do not interact with or target eukaryotic cell membranes (Figure 6).

Retained Antimicrobial Activity Indicates That ASU2060 Is Stable in Human Serum. To assess the vulnerability of ASU2060 to human proteolytic degradation during therapeutic treatment, we exposed ASU2060 to 20% human serum for 1−24 h and subsequently analyzed ASU2060 bactericidal activity against *E. coli*. As shown in Figure 7,

https://doi.org/10.1021/acsomega.2c02844
ACS Omega 2022, 7, 23967−23977

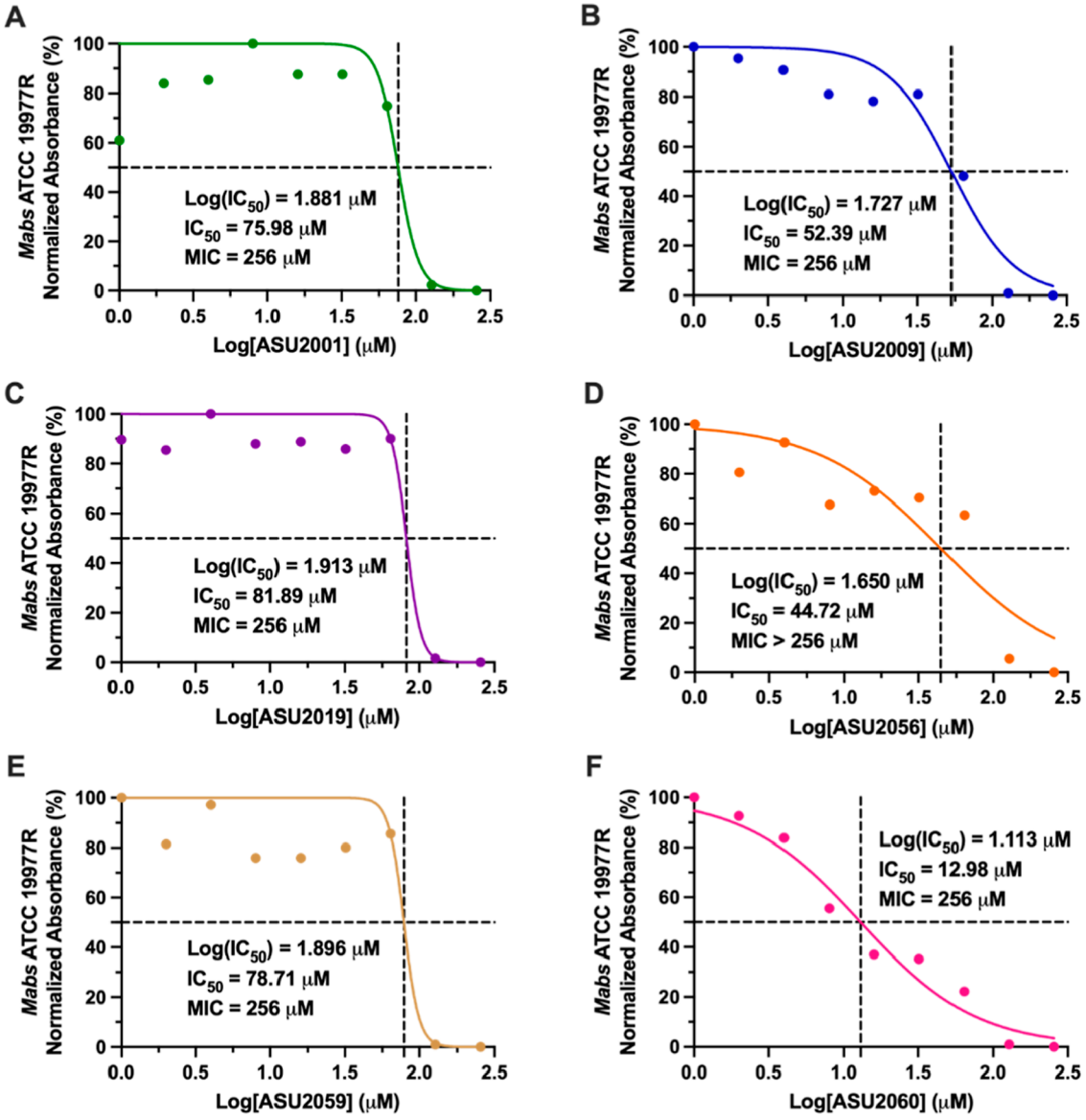

Figure 4. IC_{50} and MIC values of (A) ASU2001, (B) ASU2009, (C) ASU2019, (D) ASU2056, (E) ASU2059, and (F) ASU2060 peptides against *Mabs* ATCC 19977R rough morphotype in MHB supplemented with EDTA (100 μM) for 96 h at 37 °C. Three independent experiments were performed with the average of all three replicates plotted for each peptide. Absorbance (OD_{600}) values were normalized to the growth control (100%), and IC_{50} values were determined by nonlinear regression.

Table 1. MICs of ASU Inhibitory Peptides[a]

peptide	*Mabs* ATCC19977S MIC (μM)	*Mabs* ATCC19977R MIC (μM)	*E. coli* ATCC 25922 MIC (μM)	*P. aeruginosa* ATCC 27853 MIC (μM)	MRSA USA300 MIC (μM)
ASU2001	256	256	n.d.	n.d.	n.d.
ASU2009	256	256	n.d.	n.d.	n.d.
ASU2019	256	256	n.d.	n.d.	n.d.
ASU2056	32	>256	16	>32	>32
ASU2059	256	256	n.d.	n.d.	n.d.
ASU2060	8	256	4	8	8

[a]n.d., not determined.

ASU2060 (16 μM) retained *E. coli* bactericidal activity after preincubation with either 20% human serum or water for 24 h. This finding demonstrates ASU2060 stability and retention of antimicrobial activity in the presence of human proteases.

ASU2060 Inhibits Antibiotic-Susceptible and Multidrug-Resistant *E. coli* Clinical Isolates. We tested the efficacy of ASU2060 against six *E. coli* clinical isolates with different antibiotic resistance profiles (Table 2). The ASU2060 MIC against *E. coli* ATCC 25922 was determined to be 4 μM which was consistent with previous results (Figure 5C). *E. coli* clinical isolate 23 was susceptible to all four antibiotics (ciprofloxacin, cefazolin, ampicillin, and nitrofurantoin), where-

https://doi.org/10.1021/acsomega.2c02844
ACS Omega 2022, 7, 23967−23977

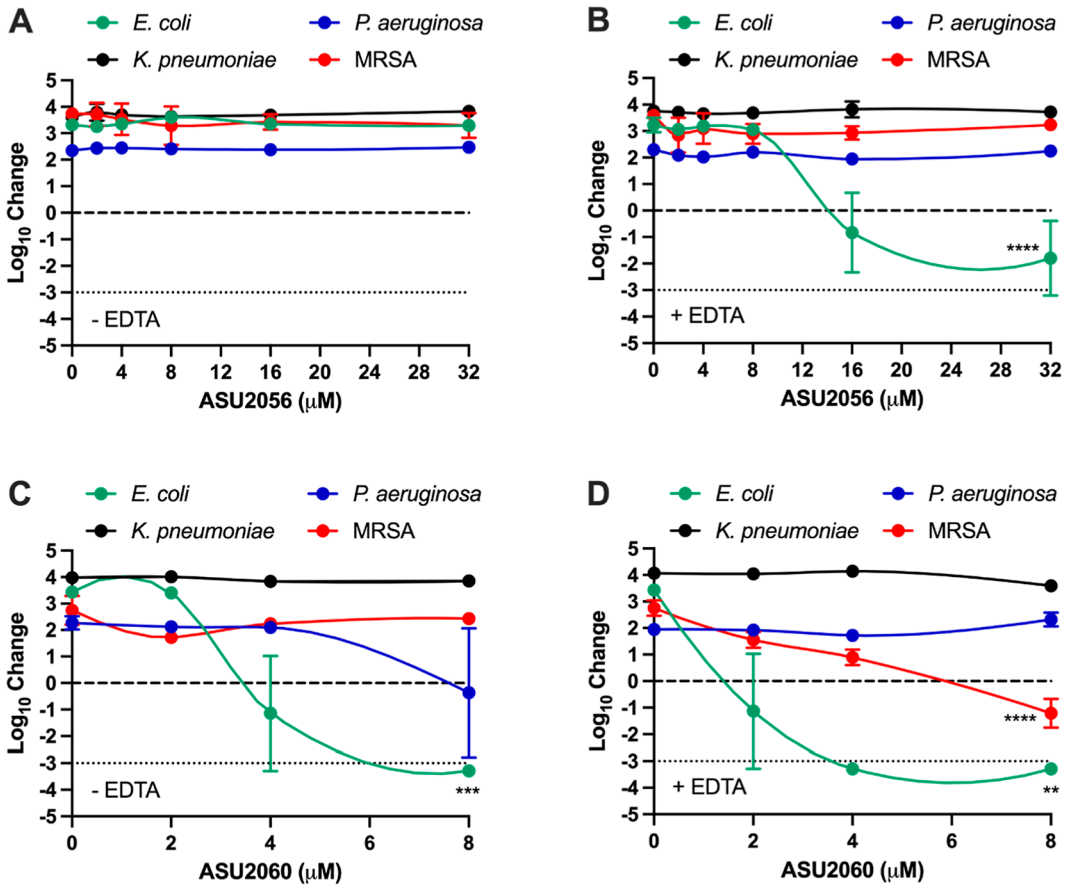

Figure 5. Antimicrobial activity of (A,B) ASU2056 and (C,D) ASU2060 peptides against *E. coli*, *K. pneumoniae*, *P. aeruginosa*, and MRSA. Peptides, at MICs determined against *Mabs* 19977S, were incubated with bacteria in MHB (B,D) with and (A,C) without 100 μM EDTA. Three independent experiments were performed with the average of all three replicates plotted and error bars representing the standard error of the mean. Log_{10} change was normalized to the initial concentration for each replicate. The dashed line indicates starting concentration, while the dotted line indicates the bactericidal threshold (99.9%). Regression analyses revealed statistically significant effects of ASU2056 or SU2060 on bacterial growth. $^{**}p < 0.01$; $^{***}p < 0.001$; and $^{****}p < 0.0001$.

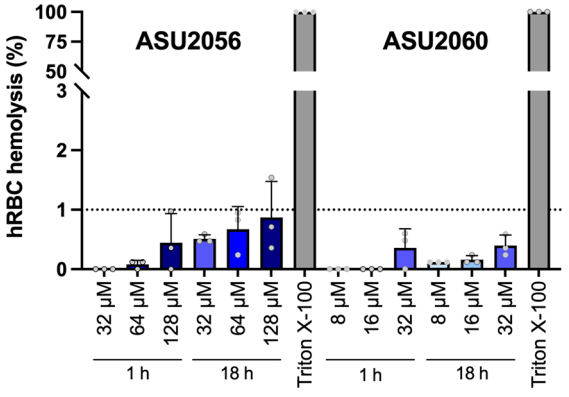

Figure 6. ASU2056 and ASU2060 peptides lack hRBC cytotoxicity. Human RBC hemolytic assays were performed with the ASU2056 and ASU2060 peptides at 1X, 2X, and 4X *Mabs* MIC concentrations with incubations of 1 and 18 h. All experiments, including Triton X-100 controls, were performed in triplicate with the bars representing the experimental mean, light gray dots representing individual biological replicates, and error bars representing the SD. The dotted line indicates 1% hRBC hemolysis.

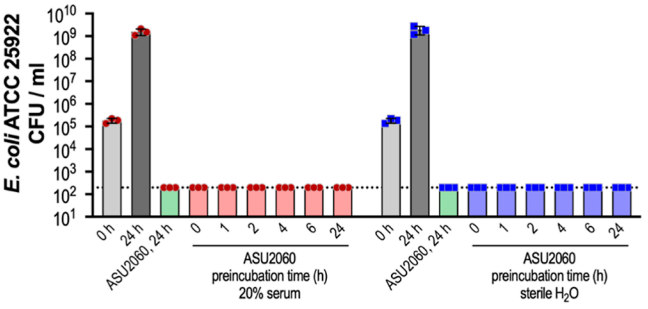

Figure 7. ASU2060 is stable in human serum and retains antibacterial activity when preincubated in human serum for 24 h. ASU2060 (16 μM; 2X MIC of *Mabs*) was preincubated in 20% pooled human serum (red bars) or sterile water (blue bars) at 37 °C prior to incubation with *E. coli* ATCC 25922 for 24 h. *E. coli* growth controls, 0 and 24 h, are shown with light gray and dark gray bars, respectively. *E. coli* incubations with ASU2060 are shown as light green bars. Individual biological replicates for the 20% serum and sterile water experiments are represented as red circles and blue squares, respectively. Data represent three independent experiments with SD.

as isolates 45 and 47 demonstrated resistance to ciprofloxacin (Table 2). *E. coli* clinical isolates 36, 97, and 98 were resistant to ciprofloxacin, cefazolin, and ampicillin (Table 2). ASU2060 inhibited all six *E. coli* clinical isolates with an MIC of 8 μM, verifying ASU2060 antimicrobial activity against clinically relevant and multidrug-resistant *E. coli* strains (Table 2).

https://doi.org/10.1021/acsomega.2c02844
ACS Omega 2022, 7, 23967−23977

Table 2. ASU2060 Inhibits Antibiotic-Resistant *E. coli* Clinical Isolates[a]

E. coli clinical isolate	Ciprofloxacin[b]	Ampicillin[c]	Cefazolin[d]	Nitrofurantoin[e]	ASU2060 MIC (μM)
23	S	S	S	S	8
45	R	S	S	S	8
47	R	S	S	S	8
36	R	R	R	S	8
97	R	R	R	S	8
98	R	R	R	S	8

[a]S = susceptible; R = resistant. [b]S $\leq$ 1 μg/mL. [c]S $\leq$ 8 μg/mL. [d]S $\leq$ 16 μg/mL. [e]S $\leq$ 64 μg/mL.

Table 3. Peptides with *Mabs* Inhibitory Activity

peptide name	peptide sequence[a]	molecular weight (Daltons)	number of positively charged residues	hydrophobicity (%)
ASU2001	QFNGrSkaAkVNFwrka	2007.37	5	41
ASU2009	rYGlSkArkVNQFrkal	2034.51	6	35
ASU2019	rVGPSAPHNlFrrkSal	1905.29	5	47
ASU2056	QrwGlSlAPYkNFrrlS	2091.50	4	41
ASU2059	YGrSArYNrrklGalSG	1924.27	5	24
ASU2060	VGrwSArYNFrwrkSGl	2138.51	5	35

[a]Lower-case letters signify D-amino acids.

DISCUSSION

Mabs is a rapidly growing NTM of particular interest because there are no effective antibiotic treatment options, particularly for lung infections.[26] This unmet need has spurred new NTM antibiotic discovery including the discovery of new AMPs. To identify novel AMP candidates, a library of random sequence peptides was screened for *Mabs* binding. The peptide microarray screening method described in this study demonstrates several important features. The flexibility of the synthesis system enables production of diverse peptide libraries, including the use of less expensive D-amino acids and other noncanonical amino acids that offer improved protease stability or side-chain diversity.[38] Also important to this method's success, the peptide libraries are random sequences, enabling screening and discovery of new, atypical, or novel cellular interactions with unique mechanisms of action. Third, the diverse phenotypic screening approach is adaptable for different microorganisms.[37,39,44] Finally, the large number of replicate microarrays produced with the photolithographic synthetic approach empowers experimental screening designs with large numbers of replicates or screening conditions. These important features and flexibility enable the design of screens that produce viable hits, even for challenging organisms, such as *Mabs*.

Mabs was screened against 125,000 synthetic peptides, containing both D- and L-amino acids, on an HD peptide microarray, identifying 79 interacting peptides,of which 6 interacting peptides were 17 amino acids long with 4−6 positively charged amino acids (Table 3). MIC assays in M7H9, CAMHB, and MHB culture media identified six peptides that inhibited *Mabs*. Reasons for why most of the peptides were not active against *Mabs* are unknown and could be due to the chemical composition of the peptides (charge, hydrophobicity, sequence, organization, D/L amino acid ratio, secondary structure, etc). Additionally, we only tested low (10 μM) and high (100 μM) concentrations of the 27 peptides, and nonactive peptides lacked anti-*Mabs* activity at the high concentration (100 μM). However, these nonactive peptides could be active at > 100 μM concentrations. The six *Mabs* inhibitory peptides that were selected for further screening were hydrophobic (24−47%), nonacidic and were rich in Arg, Val, Asn, and Phe (Table 3). The peptides (ASU2001, ASU2009, ASU2019, ASU2056, ASU2059, and ASU2060) were further screened against both *Mabs* smooth and rough morphotypes to determine the impact of cell wall glycopeptidolipids (GPLs) on activity. All six peptides displayed increased activity against the *Mabs* smooth morphotype, suggesting that interactions with cell wall GPLs are important for antibacterial activity. Additionally, all peptides exhibited increased inhibition in the presence of EDTA, further suggesting that sequestering divalent metal cations enhances peptide interactions with *Mabs*.

The two most potent peptides, ASU2056 and ASU2060, were tested for red blood cell toxicity and neither exhibited significant hRBC hemolytic activity even after prolonged incubation (18 h). ASU2060 was tested for serum stability and retained antibacterial activity after preincubation in human serum for 24 h. This level of serum stability, potent activity, along with low initial toxicity assessment suggests that ASU2060 is a strong parent scaffold for further development and activity improvement.

The phenotypic screen described here focused on a single, highly resistant mycobacterial pathogen and emphasizes the potential of phenotypic screening approaches as a discovery method for difficult-to-treat targets. Most of the known AMPs are derived from natural sources, such as frog skin secretions and toxins from other species; however, these AMPs can have unwanted side effects, such as instability and toxicity.[45] Our peptides are synthetic, contain D-amino acids to prevent proteolysis, maintain stability and antimicrobial activity after incubation with human serum, and lack toxicity against hRBCs. These identified peptides are an excellent starting point for AMP development against *Mabs*, as well as other resistant bacterial pathogens. Future directions include optimization of the two most active peptides, ASU2056 and ASU2060, to improve potency against *Mabs* while maintaining low cytotoxicity and serum stability, as well as elucidation of their mechanisms of action.

ASSOCIATED CONTENT

Supporting Information

The Supporting Information is available free of charge at https://pubs.acs.org/doi/10.1021/acsomega.2c02844.

https://doi.org/10.1021/acsomega.2c02844
ACS Omega 2022, 7, 23967−23977

Growth inhibition assays performed with the 27 unpurified, synthetic peptides against *Mabs* 19977S and *Mabs* 19977R in M7H9, CAMHB, and MHB, with and without EDTA supplementation (PDF)

AUTHOR INFORMATION

Corresponding Authors

Chris W. Diehnelt − *The Biodesign Institute Center for Innovations in Medicine, Arizona State University, Tempe, Arizona 85287, United States;* Present Address: Robust Diagnostics, Chandler, Arizona 85226, United States; orcid.org/0000-0003-4565-9338; Email: cdiehnelt@robustdiagnostics.com

Shelley E. Haydel − *School of Life Sciences and The Biodesign Institute Center for Bioelectronics and Biosensors, Arizona State University, Tempe, Arizona 85287, United States;* orcid.org/0000-0001-5542-5469; Phone: (480) 727-7234; Email: Shelley.Haydel@asu.edu

Authors

Natalie Iannuzo − *School of Life Sciences and School of Molecular Sciences, Arizona State University, Tempe, Arizona 85287, United States;* Present Address: Department of Cellular and Molecular Medicine, University of Arizona College of Medicine, Tucson, Arizona 85724, United States

Yannik A. Haller − *School of Life Sciences, Arizona State University, Tempe, Arizona 85287, United States*

Michelle McBride − *The Biodesign Institute Center for Bioelectronics and Biosensors, Arizona State University, Tempe, Arizona 85287, United States*

Sabrina Mehari − *School of Molecular Sciences, Arizona State University, Tempe, Arizona 85287, United States*

John C. Lainson − *The Biodesign Institute Center for Innovations in Medicine, Arizona State University, Tempe, Arizona 85287, United States*

Complete contact information is available at: https://pubs.acs.org/10.1021/acsomega.2c02844

Notes

The authors declare no competing financial interest.

ACKNOWLEDGMENTS

This research was supported by Research and Training Initiative seed funding provided by the ASU School of Life Sciences and C.W.D. and S.E.H. research investigator incentive accounts. N.I. was supported with an American Society for Microbiology Undergraduate Research Fellowship in 2018−2019.

REFERENCES

(1) CDC. *Antibiotic Resistance Threats in the United States, 2019*; U.S. Department of Health and Human Services: Atlanta, GA, 2019.

(2) Aminov, R. I. A brief history of the antibiotic era: lessons learned and challenges for the future. *Front. Microbiol.* **2010**, *1*, 134.

(3) Deak, D.; Outterson, K.; Powers, J. H.; Kesselheim, A. S. Progress in the fight against multidrug-resistant bacteria? A review of U.S. Food and Drug Administration-approved antibiotics, 2010-2015. *Ann. Intern. Med.* **2016**, *165*, 363−372.

(4) Mahlapuu, M.; Håkansson, J.; Ringstad, L.; Björn, C. Antimicrobial peptides: An emerging category of therapeutic agents. *Front. Cell. Infect. Microbiol.* **2016**, *6*, 194.

(5) Lei, J.; Sun, L.; Huang, S.; Zhu, C.; Li, P.; He, J.; Mackey, V.; Coy, D. H.; He, Q. The antimicrobial peptides and their potential clinical applications. *Am. J. Transl. Res.* **2019**, *11*, 3919−3931.

(6) Li, J.; Koh, J.-J.; Liu, S.; Lakshminarayanan, R.; Verma, C. S.; Beuerman, R. W. Membrane active antimicrobial peptides: Translating mechanistic insights to design. *Front. Neurosci.* **2017**, *11*, 73.

(7) Zhang, Q.-Y.; Yan, Z.-B.; Meng, Y.-M.; Hong, X.-Y.; Shao, G.; Ma, J.-J.; Cheng, X.-R.; Liu, J.; Kang, J.; Fu, C.-Y. Antimicrobial peptides: mechanism of action, activity and clinical potential. *Mil. Med. Res.* **2021**, *8*, 48.

(8) Huan, Y.; Kong, Q.; Mou, H.; Yi, H. Antimicrobial peptides: Classification, design, application and research progress in multiple fields. *Front. Microbiol.* **2020**, *11*, 582779.

(9) Benfield, A. H.; Henriques, S. T. Mode-of-action of antimicrobial peptides: Membrane disruption vs. intracellular mechanisms. *Front. Med. Technol.* **2020**, *2*, 610997.

(10) Wagner, D.; Young, L. S. Nontuberculous mycobacterial infections: a clinical review. *Infection* **2004**, *32*, 257−270.

(11) Barrow, W. W. Treatment of mycobacterial infection. *Rev. Sci. Tech.* **2001**, *20*, 55−70.

(12) Lee, M. R.; Sheng, W. H.; Hung, C. C.; Yu, C. J.; Lee, L. N.; Hsueh, P. R. Mycobacterium abscessus complex infections in humans. *Emerg. Infect. Dis.* **2015**, *21*, 1638.

(13) Jeon, K.; Kwon, O. J.; Lee, N. Y.; Kim, B.-J.; Kook, Y.-H.; Lee, S.-H.; Park, Y. K.; Kim, C. K.; Koh, W.-J. Antibiotic treatment of Mycobacterium abscessus lung disease: a retrospective analysis of 65 patients. *Am. J. Respir. Crit. Care Med.* **2009**, *180*, 896−902.

(14) Jarand, J.; Levin, A.; Zhang, L.; Huitt, G.; Mitchell, J. D.; Daley, C. L. Clinical and microbiologic outcomes in patients receiving treatment for Mycobacterium abscessus pulmonary disease. *Clin. Infect. Dis.* **2011**, *52*, 565−571.

(15) Roux, A. L.; Viljoen, A.; Bah, A.; Simeone, R.; Bernut, A.; Laencina, L.; Deramaudt, T.; Rottman, M.; Gaillard, J. L.; Majlessi, L.; Brosch, R.; Girard-Misguich, F.; Vergne, I.; de Chastellier, C.; Kremer, L.; Herrmann, J. L. The distinct fate of smooth and rough Mycobacterium abscessus variants inside macrophages. *Open Biol.* **2016**, *6* 160185. DOI: 10.1098/rsob.160185

(16) Bernut, A.; Herrmann, J. L.; Kissa, K.; Dubremetz, J. F.; Gaillard, J. L.; Lutfalla, G.; Kremer, L. Mycobacterium abscessus cording prevents phagocytosis and promotes abscess formation. *Proc. Natl. Acad. Sci. U. S. A.* **2014**, *111*, No. E943.

(17) Pawlik, A.; Garnier, G.; Orgeur, M.; Tong, P.; Lohan, A.; Le Chevalier, F.; Sapriel, G.; Roux, A.-L.; Conlon, K.; Honoré, N.; Dillies, M.-A.; Ma, L.; Bouchier, C.; Coppée, J.-Y.; Gaillard, J.-L.; Gordon, S. V.; Loftus, B.; Brosch, R.; Herrmann, J. L. Identification and characterization of the genetic changes responsible for the characteristic smooth-to-rough morphotype alterations of clinically persistent Mycobacterium abscessus. *Mol. Microbiol.* **2013**, *90*, 612−629.

(18) Jönsson, B. E.; Gilljam, M.; Lindblad, A.; Ridell, M.; Wold, A. E.; Welinder-Olsson, C. Molecular epidemiology of Mycobacterium abscessus, with focus on cystic fibrosis. *J. Clin. Microbiol.* **2007**, *45*, 1497.

(19) Rottman, M.; Catherinot, E.; Hochedez, P.; Emile, J.-F.; Casanova, J.-L.; Gaillard, J.-L.; Soudais, C. Importance of T cells, gamma interferon, and tumor necrosis factor in immune control of the rapid grower Mycobacterium abscessus in C57BL/6 mice. *Infect. Immun.* **2007**, *75*, 5898−5907.

(20) Medjahed, H.; Reyrat, J.-M. Construction of Mycobacterium abscessus defined glycopeptidolipid mutants: comparison of genetic tools. *Appl. Environ. Microbiol.* **2009**, *75*, 1331−1338.

(21) Bernut, A.; Viljoen, A.; Dupont, C.; Sapriel, G.; Blaise, M.; Bouchier, C.; Brosch, R.; de Chastellier, C.; Herrmann, J.-L.; Kremer, L. Insights into the smooth-to-rough transitioning in Mycobacterium bolletii unravels a functional Tyr residue conserved in all mycobacterial MmpL family members. *Mol. Microbiol.* **2016**, *99*, 866−883.

(22) Nessar, R.; Reyrat, J. M.; Davidson, L. B.; Byrd, T. F. Deletion of the mmpL4b gene in the Mycobacterium abscessus glycopeptidolipid biosynthetic pathway results in loss of surface colonization capability, but enhanced ability to replicate in human macrophages and stimulate their innate immune response. *Microbiology* **2011**, *157*, 1187−1195.

(23) Byrd, T. F.; Lyons, C. R. Preliminary characterization of a Mycobacterium abscessus mutant in human and murine models of infection. *Infect. Immun.* **1999**, *67*, 4700−4707.
(24) Catherinot, E.; Roux, A.-L.; Macheras, E.; Hubert, D.; Matmar, M.; Dannhoffer, L.; Chinet, T.; Morand, P.; Poyart, C.; Heym, B.; Rottman, M.; Gaillard, J.-L.; Herrmann, J.-L. Acute respiratory failure involving an R variant of Mycobacterium abscessus. *J. Clin. Microbiol.* **2009**, *47*, 271−274.
(25) Davidson, L. B.; Nessar, R.; Kempaiah, P.; Perkins, D. J.; Byrd, T. F. Mycobacterium abscessus glycopeptidolipid prevents respiratory epithelial TLR2 signaling as measured by HbetaD2 gene expression and IL-8 release. *PLoS One* **2011**, *6*, No. e29148.
(26) Griffith, D. E.; Aksamit, T.; Brown-Elliott, B. A.; Catanzaro, A.; Daley, C.; Gordin, F.; Holland, S. M.; Horsburgh, R.; Huitt, G.; Iademarco, M. F.; Iseman, M.; Olivier, K.; Ruoss, S.; von Reyn, C. F.; Wallace, R. J., Jr.; Winthrop, K.; Subcommittee, A. T. S. M. D. American Thoracic Society; Infectious Disease Society of America, An official ATS/IDSA statement: diagnosis, treatment, and prevention of nontuberculous mycobacterial diseases. *Am. J. Respir. Crit. Care Med.* **2007**, *175*, 367−416.
(27) Namkoong, H.; Kurashima, A.; Morimoto, K.; Hoshino, Y.; Hasegawa, N.; Ato, M.; Mitarai, S. Epidemiology of pulmonary nontuberculous mycobacterial disease, Japan. *Emerg. Infect. Dis.* **2016**, *22*, 1116−1117.
(28) Vinnard, C.; Longworth, S.; Mezochow, A.; Patrawalla, A.; Kreiswirth, B. N.; Hamilton, K. Deaths related to nontuberculous mycobacterial infections in the United States, 1999-2014. *Ann. Am. Thorac. Soc.* **2016**, *13*, 1951−1955.
(29) Nessar, R.; Cambau, E.; Reyrat, J. M.; Murray, A.; Gicquel, B. Mycobacterium abscessus: a new antibiotic nightmare. *J. Antimicrob. Chemother.* **2012**, *67*, 810−818.
(30) Greendyke, R.; Byrd, T. F. Differential antibiotic susceptibility of Mycobacterium abscessus variants in biofilms and macrophages compared to that of planktonic bacteria. *Antimicrob. Agents Chemother.* **2008**, *52*, 2019−2026.
(31) Ballarino, G. J.; Olivier, K. N.; Claypool, R. J.; Holland, S. M.; Prevots, D. R. Pulmonary nontuberculous mycobacterial infections: antibiotic treatment and associated costs. *Respir. Med.* **2009**, *103*, 1448−1455.
(32) Koh, W.-J.; Jeong, B.-H.; Kim, S.-Y.; Jeon, K.; Park, K. U.; Jhun, B. W.; Lee, H.; Park, H. Y.; Kim, D. H.; Huh, H. J.; Ki, C.-S.; Lee, N. Y.; Kim, H. K.; Choi, Y. S.; Kim, J.; Lee, S.-H.; Kim, C. K.; Shin, S. J.; Daley, C. L.; Kim, H.; Kwon, O. J. Mycobacterial characteristics and treatment outcomes in Mycobacterium abscessus lung disease. *Clin. Infect. Dis.* **2017**, *64*, 309−316.
(33) Fellner, R. C.; Terryah, S. T.; Tarran, R. Inhaled protein/peptide-based therapies for respiratory disease. *Mol. Cell Pediatr.* **2016**, *3*, 16.
(34) Falkinham, J. O., 3rd Epidemiology of infection by non-tuberculous mycobacteria. *Clin. Microbiol. Rev.* **1996**, *9*, 177−215.
(35) Adjemian, J.; Olivier, K. N.; Seitz, A. E.; Holland, S. M.; Prevots, D. R. Prevalence of nontuberculous mycobacterial lung disease in U.S. Medicare beneficiaries. *Am. J. Respir. Crit. Care Med.* **2012**, *185*, 881−886.
(36) Legutki, J. B.; Zhao, Z. G.; Greving, M.; Woodbury, N.; Johnston, S. A.; Stafford, P. Scalable high-density peptide arrays for comprehensive health monitoring. *Nat. Commun.* **2014**, *5*, 3785.
(37) Domenyuk, V.; Loskutov, A.; Johnston, S. A.; Diehnelt, C. W. A technology for developing synbodies with antibacterial activity. *PLoS One* **2013**, *8*, No. e54162.
(38) Diehnelt, C. W. Peptide array based discovery of synthetic antimicrobial peptides. *Front. Microbiol.* **2013**, *4*, 402.
(39) Johnston, S. A.; Domenyuk, V.; Gupta, N.; Batista, M. T.; Lainson, J. C.; Zhao, Z.-G.; Lusk, J. F.; Loskutov, A.; Cichacz, Z.; Stafford, P.; Legutki, J. B.; Diehnelt, C. W. A simple platform for the rapid development of antimicrobials. *Sci. Rep.* **2017**, *7*, 17610.
(40) Zhang, F.; Jiang, J.; McBride, M.; Yang, Y.; Mo, M.; Iriya, R.; Peterman, J.; Jing, W.; Grys, T.; Haydel, S. E.; Tao, N.; Wang, S. Direct antimicrobial susceptibility testing on clinical urine samples by optical tracking of single cell division events. *Small* **2020**, *16*, No. e2004148.
(41) Mo, M.; Yang, Y.; Zhang, F.; Jing, W.; Iriya, R.; Popovich, J.; Wang, S.; Grys, T.; Haydel, S. E.; Tao, N. Rapid antimicrobial susceptibility testing of patient urine samples using large volume free-solution light scattering microscopy. *Anal. Chem.* **2019**, *91*, 10164−10171.
(42) Zhang, F.; Jiang, J.; McBride, M.; Zhou, X.; Yang, Y.; Mo, M.; Peterman, J.; Grys, T.; Haydel, S. E.; Tao, N.; Wang, S. Rapid antimicrobial susceptibility testing on clinical urine samples by video-based object scattering intensity detection. *Anal. Chem.* **2021**, *93*, 7011−7021.
(43) Rüger, K.; Hampel, A.; Billig, S.; Rücker, N.; Suerbaum, S.; Bange, F.-C. Characterization of rough and smooth morphotypes of Mycobacterium abscessus isolates from clinical specimens. *J. Clin. Microbiol.* **2014**, *52*, 244−250.
(44) Lainson, J. C.; Daly, S. M.; Triplett, K.; Johnston, S. A.; Hall, P. R.; Diehnelt, C. W. Synthetic antibacterial peptide exhibits synergy with oxacillin against MRSA. *ACS Med. Chem. Lett.* **2017**, *8*, 853−857.
(45) Chen, C. H.; Lu, T. K. Development and challenges of antimicrobial peptides for therapeutic applications. *Antibiot.* **2020**, *9*, 24.

https://doi.org/10.1021/acsomega.2c02844
ACS Omega 2022, 7, 23967−23977